

**Title:**

**Polarization enhanced two-photon excited fluorescence contrast by shaped laser pulses using a deformable phase plate**

**Author(s):**

Syed Shakir Ashraf Shah Bukhari, Ayan Halder, and Albrecht Lindinger

Document type: Postprint

Terms of Use: Copyright applies. A non-exclusive, non-transferable and limited right to use is granted. This document is intended solely for personal, non-commercial use.

**Citation:**

"Syed Shakir Ashraf Shah Bukhari, 2023, Applied Optics Vol. 62, Issue 31, pp. 8242-8247 ; <https://doi.org/10.1364/AO.503531>"  
Archiviert unter: <http://dx.doi.org/10.17169/refubium-43042>

# Polarization enhanced two-photon excited fluorescence contrast by shaped laser pulses using a deformable phase plate

SYED SHAKIR ASHRAF SHAH BUKHARI, AYAN HALDER, AND ALBRECHT LINDINGER \*

**Abstract:** We utilize spatially and temporally tailored laser pulses for polarization enhanced two-photon excited fluorescence contrasts of dyes. The shaped laser pulses are produced by first passing through a temporal pulse shaper and then through a novel two-dimensional spatial pulse shaper with deformable phase plates. Different spatial beam profiles are presented which demonstrate the potential of the new spatial pulse shaper. Particularly, a polarization enhanced fluorescence contrast between two dyes is reported by utilizing specific phase shaping in perpendicular polarization directions. The tailored laser pulses are further modified by the deformable phase plate and a polarization increased depth-dependent contrast is achieved. This spatial shaping for all polarization directions demonstrates the advantage of deformable phase plate spatial shapers compared to liquid crystals, where only one polarization direction can spatially be modified. The described polarization contrast method allows for three-dimensional scanning of probes and provides new perspectives for biophotonic applications.

## 1. Introduction

In the last years laser pulse shaping has evolved to a various tool for several research fields such as optimal control [1–4], nanooptics [5], and control of biomolecules [6]. Thereto, Fourier domain shaping with liquid crystal modulators was used resulting in temporally shaped light fields and furthermore in the modification of the light polarization which extends the pulse shaping possibilities [7–9]. Tailored laser pulses were also employed for multiphoton excited fluorescence [10], whereby intrapulse interference was utilized to selectively excite differing molecules. This approach has lead to three-dimensional imaging in multiphoton microscopy [11, 12].

Spatial modification of the laser beam profile can be conducted by using a two-dimensional modulator and corresponding focussing lenses [13]. It is carried out by liquid crystal modulators [14], or recently by a deformable phase plate modulator [15], whereby the employed phase modulations lead to desired beam shapes in the focal plane. Such spatially tailored beam profiles were employed for deep tissue focussing [16], high resolved spatial imaging [17], and microstructuring [18]. First attempts were undertaken to combine temporal and spatial shaping [19–22], because these entirely tailored pulses enable to steer photo-induced processes concurrently in time and space.

Here, simultaneously temporally and spatially polarization shaped laser pulses are employed to achieve two-photon excited fluorescence of dyes. The studies are performed with a particularly developed shaping setup first including a temporal pulse shaper and then a spatial modulator having a deformable phase plate. Initially, phase scans for different polarization conditions are presented, which indicate an increased fluorescence contrast for polarization shaped pulses compared to linear polarized pulses. Then, depth-dependent measurements are conducted by additionally using the deformable phase plate modulator. These experiments are analyzed regarding fluorescence contrasts depending on polarization states. The described pulse shaping technique exhibits novel perspectives for biophotonic applications.

## 2. Experimental

The experimental setup is schematically presented in Fig. 1. A Nd:YVO<sub>4</sub> laser (Verdi V, Coherent, Inc.) pumps a titanium sapphire laser oscillator (MIRA, Coherent Inc) having an average power of 500 mW, a pulse duration of 70 fs, and a repetition rate of 76 MHz. The central wavelength is adjusted to 800 nm with a full width at half maximum of approximately 25 nm. The generated fs-laser pulses pass a 4f pulse shaper having a computer controlled liquid crystal light modulator (SLM 640, Cambridge Research Instruments) with optical axes at  $\pm 45^\circ$  to the horizontal which allows for shaping the phase and polarization of the laser light. A half-wave plate is placed after the modulator in order to rotate the light field by  $45^\circ$  that the light components modified by the liquid crystals are turned to horizontal and vertical direction, respectively. Such temporally shaped laser pulses are then guided through a deformable phase plate wavefront modulator (Delta 7, Phaseform GmbH) being used as a 2D spatial beam shaper in this experimental setup. The deformable phase plate has an electrode array within the active area having a diameter of 10 mm. It is an active device designed to locally change the optical path length, the geometric length times refractive index, traveled by light. This transmissive device is less than 1 mm thick and consists of a sealed liquid filled volume with a flexible polymeric membrane on one side and a rigid, transparent glass substrate on the other. The volume between the membrane and the substrate is filled with a high-refractive-index liquid. The conductive membrane is pulled toward the substrate when a voltage is applied to the electrodes. This actuation displaces the liquid, and changes the effective optical path length of light that refracts through the wavefront modulator. All polarization components can equally be shaped with this modulator.

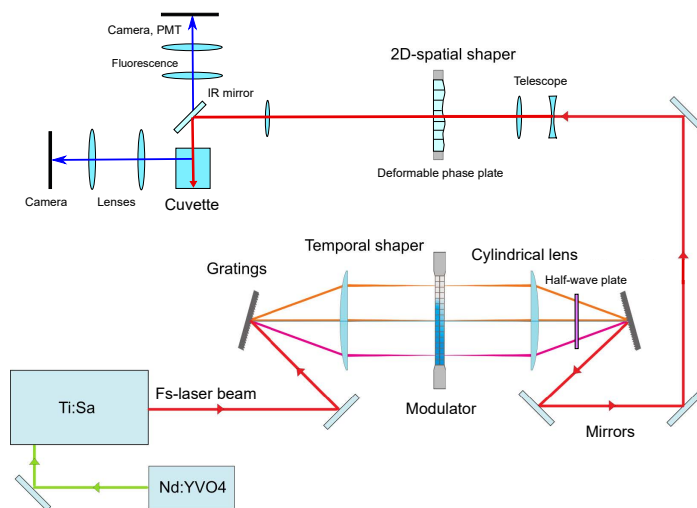


Fig. 1. Schematic experimental setup including a fs-laser (Ti:Sa), a temporal pulse shaper with gratings and a liquid crystal light modulator, and a spatial beam shaper utilizing a 2D deformable phase plate. Furthermore, a cuvette for fluorescence excitation and optical components for detection are depicted. The laser beam is first guided through the temporal pulse shaper, then through the spatial pulse shaper, and finally it is focused into a cuvette. After passing collecting lenses the fluorescence is detected in perpendicular directions, either by cameras or a photomultiplier.

The laser beam profile is enlarged by a telescope before the spatial shaper in order to use the entire active range of the deformable phase plate. A focussing lens ( $f = 60$  mm) is located behind it to focus the laser beam into a cuvette for generating spatially modulated focal profiles.

69 A dielectric mirror for wavelengths around 800 nm is further placed before the cuvette in order  
70 to reflect the laser beam into the cuvette, while the fluorescence light passes the mirror (see  
71 Fig. 1). This top view geometry enables simultaneous excitation and detection on the surface  
72 normal. The cuvette is filled with the laser dyes coumarin 102 (c102) or coumarin 120 (c120)  
73 (received from Radiant Dyes) dispersed in highly viscous glycerol. The generated two-photon  
74 excited fluorescence passes an IR glass filter (BG 39) and is directed on cameras (Logitec) or  
75 a photomultiplier (Hamamatsu). The IR bandpass filter [23] is used to reduce the laser stray  
76 light in order to measure only the fluorescence signals. The fluorescence images are taken in  
77 side and top view configuration where the detectors face the side or front surface of the cuvette,  
78 respectively. Before starting the measurements, suitable phase functions are inscribed on the  
79 temporal modulator to achieve a short pulse resulting in a constant phase which is a prerequisite  
80 for the phase-controlled measurements.

### 81 3. Results

#### 82 3.1. Two-photon excited fluorescence by polarization tailored pulses

83 The present pulse shaper setup allows for generating polarization shaped pulses with independently  
84 tailored perpendicular polarization components. This is conducted by separately inscribing  
85 the corresponding voltages on the two liquid crystal arrays of the temporal modulator which  
86 have perpendicularly arranged optical axes and leads to independent phase shaping of the  
87 two perpendicular polarization components. The half-wave plate located behind the temporal  
88 modulator turns the light field by  $45^\circ$  in order to orient the light components shaped by the  
89 liquid crystals to the horizontal and vertical direction, respectively. This is done to prevent the  
90 second polarization dependent grating from changing the angle between the shaped polarization  
91 components. The subsequent spatial modulator does not modify the polarization directions. The  
92 two-photon excited fluorescence for such pulses is recorded for coumarin 102 and coumarin 120,  
93 respectively.

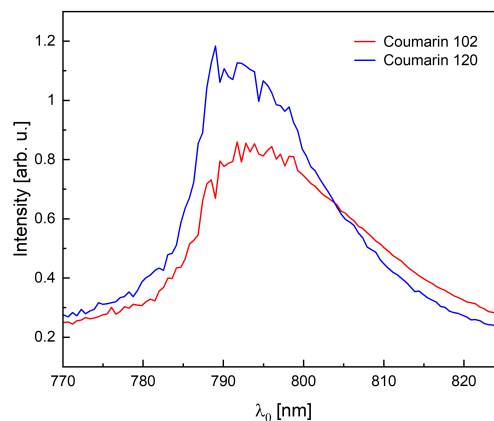


Fig. 2. Two-photon excited fluorescence signals by scanning the excitation phase center wavelength are presented for coumarin 102 (red) and coumarin 120 (blue) generated for perpendicularly polarized subpulses. Third order phase scans of the first subpulse were performed and the fluorescence was recorded behind a horizontally oriented polarizer. A red-shift of the curve for coumarin 102 compared to coumarin 120 is obtained.

94 The two perpendicularly oriented polarization components can further be phase-shaped  
95 to obtain selective two-photon excitations. Antisymmetric third order phase functions are  
96 used to receive spectrally narrow two-photon excited fluorescence maxima due to constructive

97 interference, similar as described in [10]. Phase functions  $\phi(\omega) = \frac{b_3}{6}(\omega - \omega_0)^3$  with a third order  
98 phase factor  $b_3$  and differently tuned phase center frequencies  $\omega_0$  are independently inscribed on  
99 the perpendicular polarization components of the temporal pulse shaper. The phase center value  
100 is thereby stepwise moved from lower to higher wavelengths by inscribing the corresponding  
101 voltage values on the modulator. Constructive interference close to  $\omega_0$  results in spectrally narrow  
102 two-photon maxima and enables two-photon excited fluorescence contrast enhancement.

103 Fig. 2 shows the two-photon excited fluorescence of coumarin 102 and coumarin 120,  
104 respectively, for a wavelength scan of  $\lambda_0 = 2\pi c/\omega_0$  with a phase factor of  $b_3 = 5 \cdot 10^5 \text{ fs}^3$  of  
105 the first horizontally polarized subpulse. This is done in the top-view geometry, where the  
106 photomultiplier faces the cuvette wall of the laser entrance (see Fig. 1). A horizontally oriented  
107 polarizer is thereby placed in the fluorescence path. A red-shift of coumarin 102 signals compared  
108 to coumarin 120 can be observed, where a value of  $1.8 \pm 0.8 \text{ nm}$  was found for the red-shift by  
109 calculating the difference of the arithmetic means of the two curves. This can be rationalized  
110 by a higher two-photon absorption cross-section of coumarin 102 relative to coumarin 120 by  
111 proceeding to larger wavelengths. Contrast curves can be determined from the scan data.

### 112 3.2. Contrast enhancement with polarization shaped pulses

113 The two-photon excited fluorescence characteristics by polarization-shaped laser pulses is  
114 investigated for different polarization conditions. Thereto, a polarizer is placed at different  
115 positions and the results are compared. The fluorescence yield is influenced by antisymmetric  
116 third order phase functions inscribed on the temporal pulse shaper which lead to constructive  
117 two-photon excited fluorescence close to the antisymmetry wavelength of the phase function.  
118 The applied laser pulses consist of two perpendicularly polarized subpulses with a time delay  
119 of 400 fs. The first horizontally polarized subpulse exhibits a third order phase with a phase  
120 factor of  $b_3 = 5 \cdot 10^5 \text{ fs}^3$  and the antisymmetry point will be spectrally scanned. The second  
121 vertically polarized subpulse has a third order phase with a phase factor of  $b_3 = 5 \cdot 10^4 \text{ fs}^3$ , an  
122 antisymmetry wavelength of  $\lambda_0 = 790 \text{ nm}$ , and is kept constant during the measurement.

123 In Fig. 3 the center wavelength of the third order phase is scanned for the first subpulse. The  
124 contrasts  $c = (I_{c102} - I_{c120}) / (I_{c102} + I_{c120})$  of third order phase center wavelength scans with  
125 different polarization adjustments are presented, where  $I_{c102}$  and  $I_{c120}$  indicate the fluorescence  
126 intensities of coumarin 102 and 120, respectively. The measurements were performed with  
127 horizontally or vertically oriented polarizer in the fluorescence path and with a polarizer placed  
128 in the laser excitation path, oriented at  $45^\circ$  to the horizontal, which delivers a linearly polarized  
129 laser pulse with two delayed sub pulses. The recorded data allow for a comparison between  
130 polarization-shaped and linear polarized laser pulses. The maximal contrast difference of the  
131 data with vertical polarizer ( $\Delta c = 0.12$ ) is smaller than for the linearly polarized case ( $\Delta c = 0.2$ ),  
132 whereas the contrast difference for the horizontal polarizer is larger ( $\Delta c = 0.3$ ). This indicates  
133 the dependency on polarization and proves that the contrast difference can be enhanced by  
134 polarization shaped pulses.

135 A further experiment was performed in order to explore the polarization-dependent contrast.  
136 Two perpendicularly polarized subpulses were generated, where the first exhibits a phase factor of  
137  $b_3 = 5 \cdot 10^5 \text{ fs}^3$  and an antisymmetry wavelength of  $\lambda_0 = 812 \text{ nm}$ , and the second with the same  
138 properties as explained above. The left hand inset from Fig. 3 shows a schematic 3D-image of  
139 the polarization shaped pulse. Two-photon excited fluorescence measurements were performed  
140 for both dyes, whereby the polarizer in the fluorescence path was turned in order to receive  
141 polarization-dependent data. The right hand inset of Fig. 3 displays the two-photon excited  
142 fluorescence contrast between coumarin 102 and coumarin 120 by tuning the polarizer angle  
143 relative to the horizontal. A maximum at  $0^\circ$  and a minimum close to  $90^\circ$  is obtained. This  
144 indicates that coumarin 102 is predominantly excited by the horizontally polarized subpulse and  
145 coumarin 120 by the vertically polarized subpulse. It is in agreement with the phase scan results

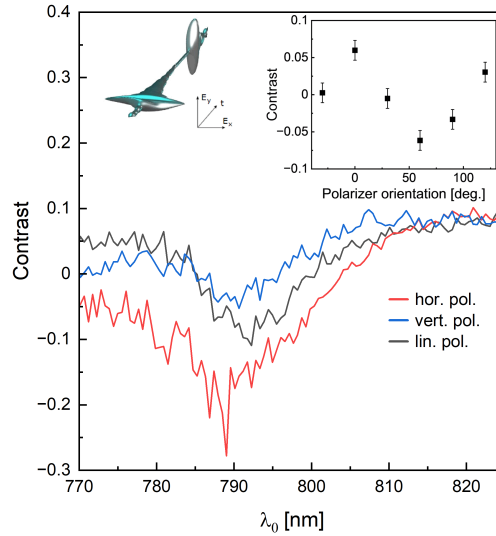


Fig. 3. Contrast curves between coumarin 102 and 120 for third order phase center wavelength scans with different polarization conditions. The measurements were conducted for polarization-tailored pulses with two subpulses, whereby a horizontally (red) or vertically (blue) oriented polarizer is located in the fluorescence path. By placing a polarizer in the laser path, contrast data of a linearly polarized laser pulse (black) were generated. A polarization dependence of the maximal contrast difference is obtained and an enhanced contrast difference for polarization-shaped pulses is received. The left hand inset shows a schematic 3D-image of the polarization shaped pulse. The right hand inset displays the two-photon excited fluorescence contrast by rotating the polarizer in the fluorescence path. A maximum at the horizontal and a minimum close to the vertical direction is observed which indicates that coumarin 102 is selectively excited by the horizontally polarized subpulse and coumarin 120 by the vertically polarized subpulse.

146 from Fig. 3 and shows that one dye is selectively excited in one polarization direction and the  
 147 other dye in the other polarization direction. This can be regarded as a polarization enhanced  
 148 two-photon excited fluorescence contrast.

### 149 3.3. Spatially shaped fluorescence structures generated by a deformable phase plate 150 modulator

151 Spatially tailored laser profiles can be generated by the deformable phase plate modulator  
 152 located behind the temporal pulse shaper. Computer-controlled voltage values are applied  
 153 on the individual modulator elements to modify their thickness, and Zernike polynomials are  
 154 used for phase control which leads to spatial modulation in the focal plane of the convex lens  
 155 behind the modulator. Zernike polynomials are used in optics e.g. to describe wave front  
 156 aberrations. They have a polynomial radial and an azimuthal angular part and are separated  
 157 into even  $Z_n^m(\rho, \phi) = R_n^m(\rho)\cos(m\phi)$  and odd  $Z_n^{-m}(\rho, \phi) = R_n^m(\rho)\sin(m\phi)$  functions, with the  
 158 radius  $\rho$  and the azimuthal angle  $\phi$ . In the following the value multiplied with the Zernike  
 159 polynomial will be called prefactor.

160 Fig. 4 shows the astigmatic influence of different Zernike polynomials. Solely for this  
 161 experiment, a screen is placed at the position of the cuvette and photos of the beam profiles were  
 162 taken. The spot can be e.g. elliptically shaped by  $Z_2^2$  polynomials (Fig. 4 (b) and (c)) or by  $Z_2^{-2}$   
 163 polynomials (Fig. 4 (d) and (e)). It can be observed that the profiles are elliptically shaped with

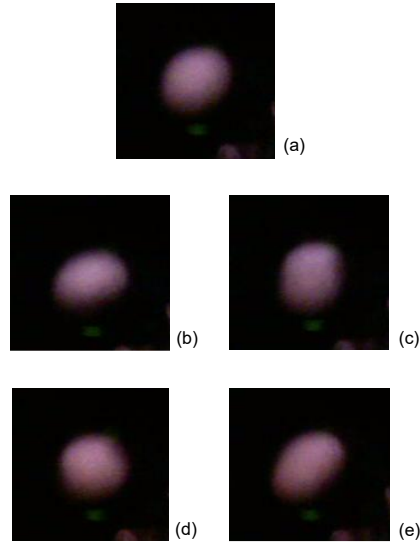


Fig. 4. Beam profiles for different Zernike polynomials. The images display the light intensities on a screen without spatial shaping (a) and with astigmatic spatial phase shaping by a  $Z_2^2$ -Zernike polynomial with the prefactors 5 (b) and -5 (c), and by a  $Z_2^{-2}$ -Zernike polynomial with the prefactors 5 (d) and -5 (e).

164 horizontal (b), vertical (c),  $+45^\circ$  (d), and  $-45^\circ$  (e) main axes which is in agreement with the  
 165 expected astigmatic outcomes.

166 Particularly, the two-photon excited fluorescence structure can be modified by forming the beam  
 167 profile. This is demonstrated by moving the focal depth position with  $Z_2^0$ -Zernike polynomials.  
 168 Fluorescence images are presented in Fig. 5 where two adjacent cuvettes are observed from the  
 169 side with coumarin 102 filled in the left (rear) and coumarin 120 in the smaller right (front)  
 170 cuvette. The green fluorescing focus is located in the rear cuvette by using a prefactor of -5 and  
 171 the blue fluorescing focus in the front cuvette with a prefactor of 5. These measurements were  
 172 conducted with short pulses having a constant spectral phase.

### 173 3.4. Depth-dependent two-photon excited fluorescence of polarization shaped pulses

174 A good contrast between different substances on small distances is important for fluorescence  
 175 imaging. Here, this goal will be approached by simultaneous temporally and spatially tailored  
 176 pulses in order to perform selective depth-dependent two-photon excitations of different dyes.  
 177 Hence, a depth-dependent contrast measurement with polarization-shaped pulses is conducted.  
 178 The employed pulses exhibit a first horizontally polarized subpulse with a third order phase  
 179 factor of  $b_3 = 5 \cdot 10^5 \text{ fs}^3$  and an antisymmetry wavelength of  $\lambda_0 = 812 \text{ nm}$ , and a 400 fs delayed  
 180 second vertically polarized subpulse with a third order phase factor of  $b_3 = 5 \cdot 10^4 \text{ fs}^3$  and an  
 181 antisymmetry wavelength of  $\lambda_0 = 790 \text{ nm}$ . The polarized pulse focus is moved by about 2 mm  
 182 (see Fig. 5) from one cuvette to the other by tuning the prefactor of the  $Z_2^0$ -Zernike polynomial,  
 183 and the fluorescence is measured on the front side. The front cuvette is filled with coumarin 120  
 184 and the rear cuvette with coumarin 102. This order is favorable because the lower frequency  
 185 fluorescence from the rear cuvette will not be absorbed by the front cuvette, whereas absorption  
 186 would occur the other way around.

187 The experiment is again conducted with a horizontally or vertically oriented polarizer in the  
 188 fluorescence path and with a polarizer in the laser path, oriented at  $45^\circ$  to the horizontal, the

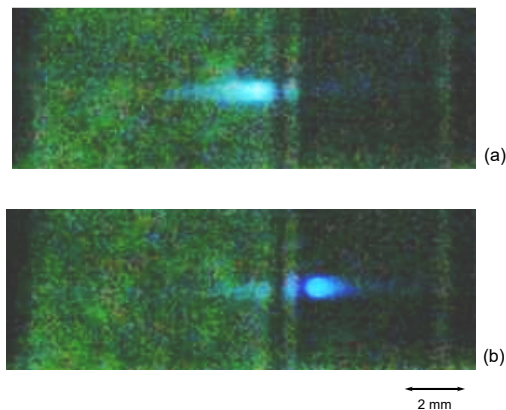


Fig. 5. Modification of the focal depth position by the  $Z_2^0$ -Zernike polynomial. Two adjacent cuvettes are visible from the side with coumarin 102 filled in the left (rear) and coumarin 120 in the smaller right (front) cuvette. The focus is located in the rear cuvette by using a prefactor of -5 (a) and it is moved to the front cuvette by a prefactor of 5 (b).

189 latter leading to a linearly polarized laser pulse. The two-photon excited fluorescence data for the  
 190 three different polarization conditions are shown in Fig. 6. The dip in the curves close to zero can  
 191 be explained by reduced fluorescence due to the cuvette walls. At these focus positions both dyes  
 192 may contribute to the signal since the focal range is partially present in both cuvettes. The lower  
 193 intensity of the vertical compared the horizontal component can be explained by the reduced  
 194 reflection of the second grating in the temporal modulator for vertical polarization. Particularly  
 195 for the horizontally oriented polarizer, an enhanced signal ratio is obtained for the rear to the  
 196 front cuvette compared to the linearly polarized pulse and a reduced ratio is observed for the  
 197 vertically oriented polarizer. The corresponding contrast for the horizontal case of 0.06 is hence  
 198 increased compared to the contrast of 0.03 for the linearly polarized case, and the contrast for  
 199 the vertical case is decreased to -0.02. This demonstrates that the spatially dependent contrast  
 200 can be enhanced by polarization shaped laser pulses. Since these polarization tailored laser  
 201 pulses can well be spatially moved by the deformable phase plate modulator, three-dimensional  
 202 scans of probes can be performed. The spatial modification without changing the polarization  
 203 state is beneficial compared to spatial shaping by liquid crystal modulators, where only a single  
 204 polarization direction can be modulated.

#### 205 4. Conclusion

206 Spatially and temporally polarization shaped laser pulses were applied for two-photon excited  
 207 fluorescence of dyes. The pulses were shaped including different polarization directions which  
 208 means that they exhibit a temporal profile, where the polarization direction is changed during the  
 209 pulse. These investigations were conducted by using a combination of a temporal pulse shaper  
 210 and a novel deformable phase plate spatial modulator. Characteristic third order phase scans  
 211 were recorded for different polarization directions. They exhibit an enhanced two-photon excited  
 212 fluorescence contrast difference for polarization shaped pulses compared to linear polarized  
 213 pulses. Moreover, different spatially modified beam profiles were presented. Particularly,  
 214 depth-dependent two-photon excited fluorescence experiments were performed by utilizing the  
 215 deformable phase plate shaper. The measurements feature an increased spatial fluorescence  
 216 contrast for specific polarization-shaped pulses compared to linearly polarized pulses. The  
 217 polarization-tailored laser pulses, which lead to increased contrast differences, can hence spatially



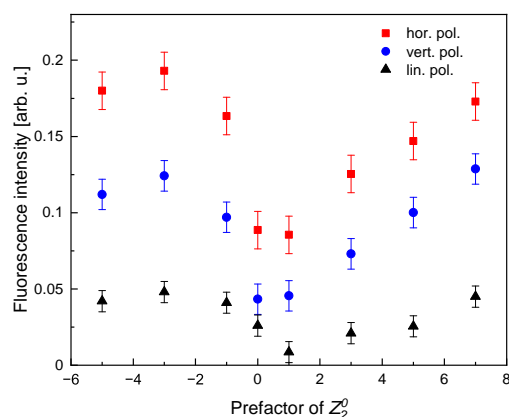


Fig. 6. Depth-dependent fluorescence for differing polarization conditions. The measurement is recorded with a horizontally (red) or vertically (blue) oriented polarizer in the fluorescence path and a polarizer in the laser path, oriented at  $45^\circ$  to the horizontal (black), which results in a linearly polarized pulse. The two-photon excited fluorescence is measured for the three polarization conditions. In horizontal direction an enhanced signal ratio is obtained for the rear to the front cuvette compared to the linearly polarized pulse and to the vertical direction which shows that the spatially dependent contrast can be increased for polarization-tailored pulses.

218 be modified by the deformable phase plate modulator. The described spatial modification for  
 219 all polarization directions is favorable compared to spatial shaping by liquid crystal modulators,  
 220 whereby only one polarization component can spatially be modulated. Since the deformable  
 221 phase plate modulator is relatively small it can well be integrated into microscopes in order to  
 222 improve the image by adaptive optics. The polarization contrast technique developed here can be  
 223 employed for three-dimensional scans of biological probes and has a high potential for imaging  
 224 applications.

225 **Acknowledgements.** The authors thank Prof. Dr. W. Kuch and the team of Phaseform GmbH for  
 226 supporting this experimental study.

227 **Disclosures.** The authors declare no conflicts of interest.

228 **Data Availability Statement.** Data underlying the results presented in this paper are not publicly available  
 229 at this time but may be obtained from the authors upon reasonable request.

## 230 References

- 231 1. A. Assion, T. Baumert, M. Bergt, T. Brixner, B. Kiefer, V. Seyfried, M. Strehle and G. Gerber, "Control of chemical  
 232 reactions by feedback-optimized phase-shaped femtosecond laser pulses," *Science*, **282**, 919-922 (1998).
- 233 2. T. Brixner and G. Gerber, "Quantum Control of Gas-Phase and Liquid-Phase Femtochemistry," *ChemPhysChem* **4**,  
 234 418-438 (2003).
- 235 3. G. Vogt, G. Krampert, P. Niklaus, P. Nuernberger and G. Gerber, "Optimal Control of Photoisomerization," *Phys.*  
 236 *Rev. Lett.* **94**, 068305 (2005).
- 237 4. A. Lindinger, C. Lupulescu, M. Plewicky, F. Vetter, A. Merli, S. M. Weber and L. Wöste, "Isotope Selective Ionization  
 238 by Optimal Control Using Shaped Femtosecond Laser Pulses," *Phys. Rev. Lett.* **93**, 033001 (2004).
- 239 5. M. Aeschlimann, M. Bauer, D. Bayer, T. Brixner, F. J. Garcia de Abajo, W. Pfeiffer, M. Rohmer, C. Spindler and F.  
 240 Steeb, "Adaptive subwavelength control of nano-optical fields," *Nature* **446**, 301-304 (2007).
- 241 6. W. Wohlleben, T. Buckup, J. L. Herek and M. Motzkus, "Coherent Control for Spectroscopy and Manipulation of  
 242 Biological Dynamics," *ChemPhysChem* **6**, 850-857 (2005).
- 243 7. L. Polachek, D. Oron, and Y. Silberberg, "Full control of the spectral polarization of ultrashort pulses," *Opt. Lett.* **31**,  
 244 631-633 (2006).
- 245 8. T. Brixner and G. Gerber, "Femtosecond polarization pulse shaping," *Opt. Lett.* **26**, 557-559 (2001).

- 246 9. F. Weise and A. Lindinger, "Full parametric pulse shaping in phase, amplitude, and polarization using an effective  
247 four-array modulator," *Appl. Phys. B* **101**, 79-91 (2010).
- 248 10. V. V. Lozovoy, I. Pastirk, K. A. Walowicz and M. Dantus, "Multiphoton intrapulse interference. II. Control of two-  
249 and three-photon laser induced fluorescence with shaped pulses," *Chem. Phys.* **118**, 3187-3196 (2003).
- 250 11. S. Perry, R. Burke and E Brown, "Two-Photon and Second Harmonic Microscopy in Clinical and Translational  
251 Cancer Research," *Ann. Biomed. Eng.* **40**, 277-291 (2012).
- 252 12. W. Denk, J. H. Strickler and W. W. Webb, "Two-photon laser scanning fluorescence microscopy," *Science* **248**, 73-76  
253 (1990).
- 254 13. C. Maurer, A. Jesacher, S. Bernet and M. Ritsch-Marte, "What spatial light modulators can do for optical microscopy,"  
255 *Laser Photonics Rev.* **5**, 81-101 (2011).
- 256 14. N. Sanner, N. Huot, E. Audouard, C. Larat and J.-P. Huignard, "Programmable focal spot shaping of amplified  
257 femtosecond laser pulses," *Opt. Lett.* **30**, 1479-1481 (2005).
- 258 15. K. Banerjee, P. Rajaeipour, C. Ataman, and H. Zappe, "Optofluidic adaptive optics," *Appl. Opt.* **57**, 6338-6344  
259 (2018).
- 260 16. A. Tanabe, T. Hibi, S. Ipponjima, K. Matsumoto, M. Yokoyama, M. Kurihara, N. Hashimoto and T. Nemoto,  
261 "Correcting spherical aberrations in a biospecimen using a transmissive liquid crystal device in two-photon excitation  
262 laser scanning microscopy," *J. Biomed. Opt.* **20**, 101204 (2015).
- 263 17. S. Hell and J. Wichmann, "Breaking the diffraction resolution limit by stimulated emission: stimulated-emission-  
264 depletion fluorescence microscopy," *Opt. Lett.* **19**, 780-782 (1994).
- 265 18. N. Sanner, N. Huot, E. Audouard, C. Larat and J.-P. Huignard, "Direct ultrafast laser micro-structuring of materials  
266 using programmable beam shaping," *Opt. Lasers Eng.* **45**, 737-741 (2007).
- 267 19. T. Feurer, J. C. Vaughan, R. M. Koehl and K. A. Nelson, "Multidimensional control of femtosecond pulses by use of  
268 a programmable liquid-crystal matrix," *Opt. Lett.* **27**, 652-654 (2002).
- 269 20. D. J. McCabe, A. Tajalli, D. R. Austin, P. Bondareff, I. A. Walmsley, S. Gigan and B. Chatel, "Spatio-temporal  
270 focusing of an ultrafast pulse through a multiply scattering medium," *Nature Communications* **2**, 447 (2011).
- 271 21. O. Katz, E. Small, Y. Bromberg and Y. Silberberg, "Focusing and compression of ultrashort pulses through scattering  
272 media," *Nature Photonics* **5**, 372-377 (2011).
- 273 22. T. Feurer, J. C. Vaughan and K. A. Nelson, "Spatiotemporal coherent control of lattice vibrational waves," *Science*  
274 **299**, 374-377 (2003).
- 275 23. Schott AG, "Product sheet of the optical bandpass filter BG39," [https://www.schott.com/shop/  
276 advanced-optics/en/Matt-Filter-Plates/BG39/c/glass-BG39](https://www.schott.com/shop/advanced-optics/en/Matt-Filter-Plates/BG39/c/glass-BG39).